

## Branching Ratios and Magnetic Dipole Transition Probabilities in Odd- $A$ Rotational Nuclei

G. GOLDRING AND H. M. LOEBENSTEIN

*Department of Nuclear Physics, The Weizmann Institute of Science, Rehovoth, Israel*

AND

R. BARLOUTAUD

*Centre d'Etudes Nucléaires de Saclay, France*

(Received April 16, 1962)

Branching ratios have been measured for gamma radiations from the second excited level in odd- $A$  rotational nuclei. The magnetic dipole transition probability for the first member of the cascade transition could thus be measured in terms of the known electric quadrupole transition probability for the crossover transition. Results are reported for  $\text{Eu}^{153}$ ,  $\text{Gd}^{155}$ ,  $\text{Gd}^{157}$ ,  $\text{Er}^{167}$ ,  $\text{Yb}^{173}$ ,  $\text{Lu}^{175}$ ,  $\text{Hf}^{177}$ , and  $\text{Ta}^{181}$ . Electric quadrupole transition probabilities could also be determined in some cases where mixing ratios  $E2/M1$  were known. The  $M1$  and  $E2$  transition probabilities are compared with the corresponding quantities for the transition from the first excited state to the ground state. The ratios of  $M1$  transition probabilities for the two transitions are in good agreement with the values predicted for collective rotational motion. The gyromagnetic ratios of the collective motion  $g_R$  for odd- $Z$  nuclei are found to be consistently higher than the  $g_R$  for odd- $N$  nuclei.

### INTRODUCTION

THE information which has been gathered so far about magnetic dipole transition probabilities in rotational bands in deformed nuclei is much more scant and less accurate than the information concerning electric quadrupole transition probabilities. This situation is due more to experimental difficulties than to lack of interest. Indeed the most recent developments in the theory of collective rotations<sup>1</sup> are specifically concerned with  $M1$  moments of states and transitions, and the most important predictions of these theories relate to these quantities. Actually there does not even exist at present a clear-cut experimental test of the basic stipulation of the collective rotation theory that all magnetic dipole moments and transition probabilities in odd- $A$  nuclei are determined by just two parameters, usually referred to as  $g_R$  the gyromagnetic ratio of the collective motion and  $g_K$  the gyromagnetic ratio of the intrinsic motion.

Most of our present knowledge about  $M1$  transition probabilities  $B(M1)$  is based on combinations of measurements of  $E2$  transition probabilities  $B(E2)$ , and of mixing ratios  $\delta^2 = E2/M1$ . The lack of accuracy in most of these measurements, referred to above, stems from the fact that in many transitions the  $M1$  component predominates rather heavily, and under these circumstances the measurement of  $\delta^2$ , although quite accurate in itself does not provide a very satisfactory determination of the  $M1$  transition probability. A satisfactory procedure for such cases is to determine  $B(M1)$  directly from the total transition probability or level width. This may be achieved either by measuring the mean life of the appropriate level if there is but a single gamma-ray transition,<sup>2</sup> or—if the decay is complex and one

transition is the  $M1$  transition in question—by measuring branching ratios between the predominantly  $M1$  transition, and some other transition the mean life of which is known.

In odd- $A$  rotational nuclei the first two excited levels and the gamma-ray transitions between these and the ground state usually conform to the pattern indicated in Fig. 1. The branching ratio  $\gamma_1/\gamma_2$  has been measured in many cases where the level  $I+2$  was excited in Coulomb excitation. If  $B(E2)_1$  is known and  $\delta_2^2$  is known at least approximately (assuming  $\delta^2$  to be small), this measurement determines  $B(M1)_2$ . Usually however these measurements are not very reliable since the gamma ray  $\gamma_2$  is accompanied by the much more strongly excited gamma ray  $\gamma_3$  which is also close in energy, and in the spectral regions of both  $\gamma_1$  and  $\gamma_2$  there is usually considerable contribution from various background radiations.

In the experiments here described, branching ratios were measured by recording gamma rays in coincidence with inelastically scattered protons. The protons were passed through a magnetic analyzer and only those leaving the nucleus in the second excited level were accepted. The gamma-ray spectrum was limited in this

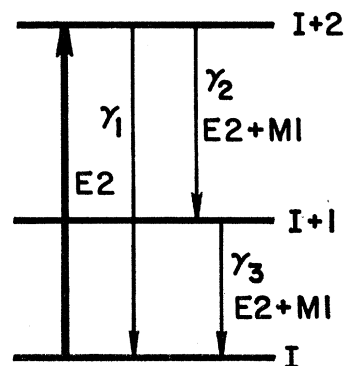


FIG. 1. The gamma-ray transitions following the excitation of the second rotational level.

<sup>1</sup> S. G. Nilsson and O. Prior, Kgl. Danske Videnskab. Selskab. Mat.-fys. Medd. 32, No. 16 (1961).

<sup>2</sup> A. E. Blaugrund, Y. Dar, and G. Goldring, Phys. Rev. 120, 1328 (1960).

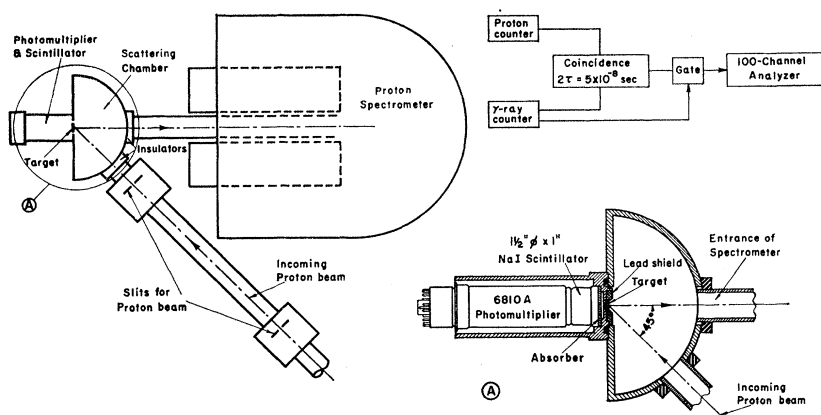


FIG. 2. Schematic drawing of the experimental arrangement.

way to radiations following the excitation of the  $I+2$  level and the analysis of the spectrum was therefore considerably simplified. A measurement of comparable accuracy and reliability is the determination of the branching ratio from conversion electron transitions following Coulomb excitation.<sup>3</sup>

If the mixing ratio  $\delta^2$  is known a branching ratio measurement determines both the  $B(M1)$  and  $B(E2)$  values, but even if  $\delta^2$  is not known the branching ratio provides a valid and accurate measurement of  $B(M1)$  in cases of predominantly  $M1$  radiation, because the  $E2$  radiation contributes in any case only a small correction in these measurements. To the low accuracy required under these conditions the  $B(E2)$  value can be inferred from other measured  $B(E2)$  values in the same band, assuming the ratios to be given by the collective motion theory. The validity of this assumption has been proved (to within the accuracy here required) by the work of Olesen and Elbek.<sup>4</sup>

Another method of measuring  $B(M1)$  strengths should be mentioned here: the measurement of angular distributions following Coulomb excitation or angular correlations involving  $\gamma_2$ . These depend linearly on  $\delta$  (in the  $E2, M1$  interference term), and since  $\delta$ , unlike  $\delta^2$ , is usually not very small, one is not confronted in this case with the problem of measuring accurately a small fraction. Unfortunately, however it seems that only on rare occasions does one find the conditions necessary for a precise measurement.

#### EXPERIMENTAL PROCEDURE

The experimental arrangement is shown in Fig. 2. Targets of odd- $A$  nuclei in the region  $153 \leq A \leq 181$  were bombarded by 3.1 to 3.4 MeV protons from the Saclay 5 MeV Van de Graaff accelerator. Inelastically scattered protons were analyzed and recorded by a double focusing magnetic spectrometer set at  $135^\circ$  to the beam, and gamma rays were recorded by a NaI scintillation counter situated immediately behind the target. The

gamma-ray spectrum gated by the scattered protons was displayed on a hundred channel analyzer.

The main problems inherent in this type of experiment are: The complete rejection of elastically scattered protons from the counting system, as these are about  $10^4$  times more prolific than the inelastic group, and achieving a reasonably high coincidence counting rate. The first condition led to the employment of magnetic analysis for the protons, and the second condition led to the requirement of high transmission in the spectrometer, large proton current and large solid angle for the gamma-ray counter.

The proton spectrometer described by Mileikowsky<sup>5</sup> was designed for a transmission of  $4.3 \times 10^{-3}$  sr and in actual practice the transmission was found to be quite close to this value. The energy resolution (full width at half maximum) was determined to a large extent by the target thickness and varied between one and two percent. A typical proton spectrum is shown in Fig. 3. It may be noticed that the general background level is so high that the inelastic groups are not at all apparent in this spectrum. Nevertheless the background counting level is low enough for this coincidence experiment. The purpose of the spectrometer is only (a) to separate the two inelastic groups, and (b) to protect the counter and coincidence circuit from the intense elastic group.

Severe restrictions are imposed in this type of experiment on the target material and the target backing.

(a) The target assembly has to be able to withstand fairly high proton currents during prolonged bombardment.

(b) The target backing has to be of such material that elastically scattered protons do not fall into the same spectral range as the inelastic groups from the target. With the spectrometer placed at  $135^\circ$  to the beam—the largest possible angle for this spectrometer—the recoil energy loss  $\Delta E_r$  is approximately given by

$$\Delta E_r/E = 3.4A/(A+1)^2,$$

<sup>3</sup> E. M. Bernstein and R. Graetzer, Phys. Rev. **119**, 1321 (1960).

<sup>4</sup> M. C. Olesen and B. Elbek, Nuclear Phys. **15**, 134 (1960).

<sup>5</sup> C. Mileikowsky, Arkiv Fysik **4**, 337 (1952); **7**, 33 (1954).

where  $E$  is the incident proton energy and  $A$  is the atomic number of the scattering nucleus. The requirement that all protons elastically scattered from the backing have energies lower than the protons inelastically scattered from the target nuclei leads to the condition:

$$3.4A_B/(A_B+1)^2 - 3.4A_T/(A_T+1)^2 > \Delta E/E, \quad (1)$$

where  $A_B$ ,  $A_T$  refer to the backing and target nuclei, respectively, and  $\Delta E$  is the target nucleus excitation energy. The highest excitation energy encountered in this experiment was 303 keV (in Ta<sup>181</sup>), and the incident proton energy varied between 3.1 and 3.5 MeV. Under these conditions relation (1) yields the condition

$$A_B < 25$$

so that only materials lighter than sodium can be used for the target backing.

(c) The intensity of gamma radiation emitted from the target backing under proton bombardment should be low. This condition is severe because of the close proximity of the gamma-ray counter to the target, and it is particularly so because the gamma radiation of the target alone leads to a high counting rate in the photomultiplier. Normally one would use high- $Z$  backing materials to satisfy this condition, but this is impossible here due to the restriction  $A_B < 25$  imposed by considerations relating to the proton detection in the spectrometer. Conditions (b) and (c) are therefore almost mutually exclusive. It was found however that carbon backings are very satisfactory on both counts. Gamma radiations from capture in carbon and from the annihilation of positrons emitted by N<sup>13</sup> are very much in evidence, but are considerably less intense than the radiation (mainly  $K$  x rays) emitted by the target for incident proton energies below 3.5 MeV. For higher bombarding energies the radiation from carbon rises rapidly beyond the permissible level, but this limitation on proton energy is not a severe restriction, as there are other considerations which preclude high bombarding energies, namely, the high ratio of  $K$  x rays to Coulomb excited gamma rays which rises rapidly with proton energy, and the comparatively high resolution required in the proton spectrometer.

The targets were in oxide form and had a thickness of a few hundred  $\mu\text{g}/\text{cm}^2$ . They were prepared by evaporation onto carbon disks, by electron bombardment, in a method similar to that described by Olesen and Elbek.<sup>4</sup> These targets proved to be very stable and showed no sign of deterioration or change after bombardment by 1  $\mu\text{A}$  of protons falling on an area of about 1-mm<sup>2</sup> for 50 h.

The gamma-ray counter consisted of a 1½-in. diam, 1-in. high NaI scintillator bounded to a type 6810A photomultiplier. The main problem encountered in the counting of gamma rays was to keep the registered spectrum free from shifts and general disturbances caused by the high counting rate. It was found that,

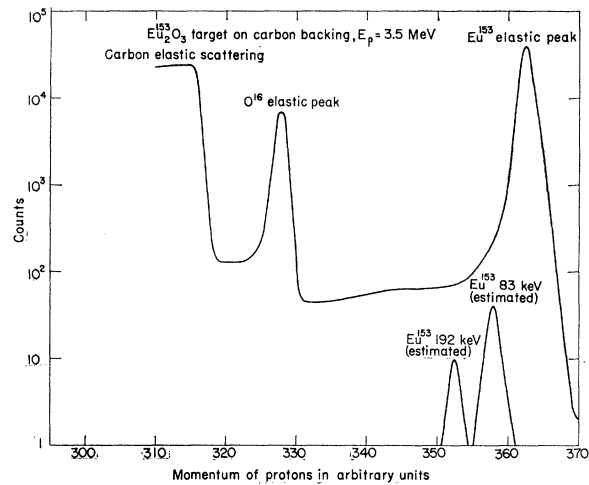


Fig. 3. Proton spectrum from Eu<sup>153</sup> target. Estimated peaks corresponding to protons exciting the first and second level are shown.

with the use of a high-current voltage divider for the photomultiplier dynodes (10 mA in the last four stages) and a linear gate similar to that described by Gabriel *et al.*,<sup>6</sup> the counting rate could be raised to  $5 \times 10^4$  counts per sec without incurring any shift or change in the gamma-ray spectrum, apart from a change of amplification in the photomultiplier. This too did not pose any serious problems provided the counting rate remained reasonably constant. The gate was fed with pulses directly from the photomultiplier anode.

As the radiation registered by the gamma-ray counter was mostly due to  $K$  x rays, the counting rate could be reduced by inserting a selective absorber in front of the counter. Tin absorbers between 36 and 290 mg/cm<sup>2</sup> in thickness were used for this purpose, reducing the x-ray intensity by factors of 1.7–9. It was not considered advisable to use thicker absorbers because such absorbers would also absorb the gamma radiation quite strongly. The absorbers were made out of several concentric circular pieces of varying radii and cemented together, so that the absorption length for the gamma rays in the tin was independent of the angle of incidence of the gamma ray on the counter.

In setting up a particular measurement the spectrometer would first be adjusted for the elastic peak, and the gated gamma-ray spectrum was recorded in a short run at this energy providing information on the random coincidence counting rate. For the proper gated gamma-ray spectrum measurement the field in the main deflection magnet of the accelerator was then raised so that the protons accepted by the spectrometer corresponded to the inelastic peak. This method of controlling the energy was found to be more convenient than changing the spectrometer field for constant bombarding energy, because the field of the deflection

<sup>6</sup> R. Gabriel, E. L. Garwin, and C. M. York, *Nuclear Instr.* **5**, 247 (1959).

magnet being uniform, could be measured with a proton resonance probe and could be controlled much more accurately and reliably than the nonuniform field of the spectrometer.

#### ANALYSIS OF THE MEASUREMENTS

The gated gamma-ray spectra following the excitation of the second excited rotational level in three typical cases  $\text{Eu}^{153}$ ,  $\text{Gd}^{155}$ , and  $\text{Lu}^{175}$  are shown in Figs. 4(a), 5, and 6. In Fig. 4(b) the ungated gamma-ray spectrum of  $\text{Eu}^{153}$  is shown together with the gamma-ray spectrum from a thick target for comparison. A gated gamma-ray spectrum from the first excited rotational state of  $\text{Eu}^{153}$  is shown in Fig. 7. In order to clarify the discussion of these spectra we give in Fig. 8 a schematic representa-

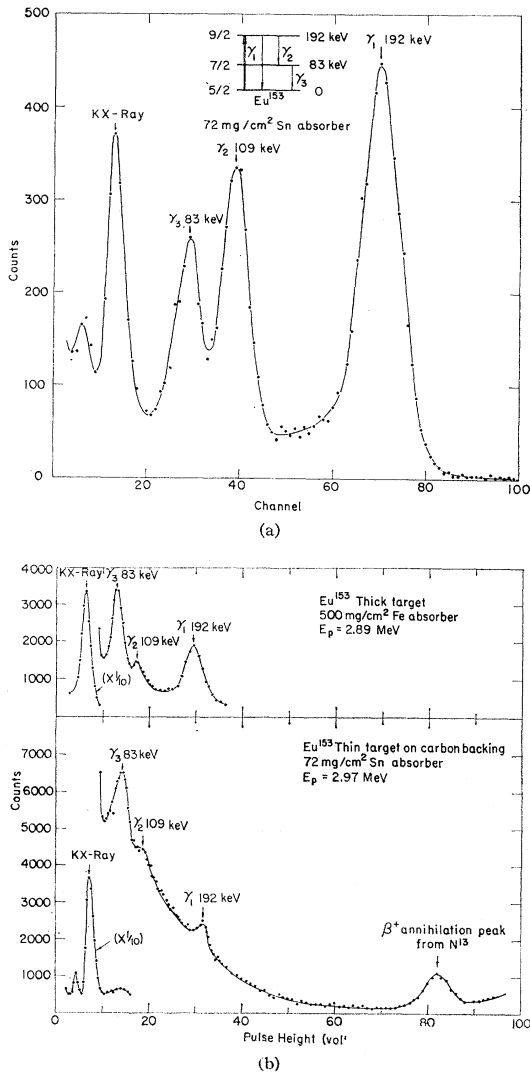


FIG. 4. (a) Gamma-ray spectrum of  $\text{Eu}^{153}$  coincident with protons which leave the nucleus in the second excited level. (b) Direct gamma-ray spectrum of  $\text{Eu}^{153}$ . Upper part: spectrum from thick target, lower part: spectrum from thin target on carbon backing.

tion:  $n(1)$ ,  $n(2)$ ,  $n(3)$  are the number of counts registered at the energies appropriate to the gamma rays  $\gamma_1$ ,  $\gamma_2$ ,  $\gamma_3$ , respectively, and  $n(4)$  are the number of recorded  $K$  x-ray counts.  $n(3')$  and  $n(4')$  are the number of gamma rays and  $K$  x rays registered following the excitation of the first excited rotational level.

As is to be expected, the great majority of all counts recorded in the gated gamma-ray spectra originate in the excitation of the level selected by the proton spectrometer. The only other sources of registered counts are random coincidences and proton bremsstrahlung.

As has been pointed out previously, random coincidences contribute appreciably to the x-ray counts  $n(4)$  and  $n(4')$ , but at all other energies they are rather unimportant and their contribution may be estimated from the counts beyond  $\gamma_1$  in Figs. 4, 5, and 6. The gated spectrum with elastic protons constitutes a fairly good measurement of random counts at all points of the gamma spectrum, the only uncertainty arising from the unknown and uncontrollable fluctuations in the beam current.

As for proton bremsstrahlung, protons which radiate a photon of energy equal to the nuclear excitation  $\Delta E$  are accepted by the spectrometer and the radiated photon will be registered in the gated spectrum at the energy of  $\gamma_1$ . The number of such events compared to, say,  $n(1)$ , is considerably smaller than the corresponding number in an ungated spectrum [as in Fig. 4(b)]. In the first place the protons scattered in this predominantly  $E1$  process are forward peaked, whereas the protons emitted in  $E2$  inelastic scattering are almost isotropic. Secondly, as will be shown in the discussion on angular distributions later on, the angular distribution of the gamma rays again favors the  $E2$  Coulomb excitation over the  $E1$  bremsstrahlung in the geometrical setup of

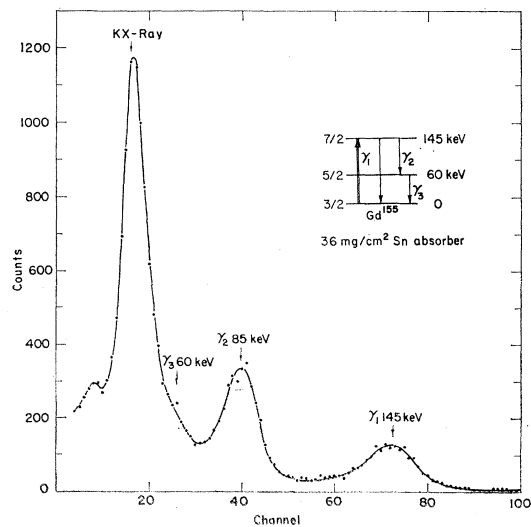


FIG. 5. Gamma-ray spectrum of  $\text{Gd}^{155}$  coincident with protons which leave the nucleus in the second excited level.

this experiment. Altogether the relative number of bremsstrahlung photons is reduced by about a factor of 4 compared to an ungated gamma-ray measurement. The contribution of bremsstrahlung to the  $\gamma_1$  peak was 0.2 to 4%, and this number could be estimated with sufficient accuracy from known data on  $B(E2)$  values and the bremsstrahlung process.

**Angular Distribution of Gamma Rays**

The angular distribution of gamma rays  $W(\theta_\gamma)$  following Coulomb excitation by protons scattered at an angle  $\theta_p$  has been given by Alder *et al.*<sup>7</sup> The formulas are much simplified if the protons are scattered in a nearly backward direction. For  $\theta_p > (3/4)\pi$  one has, to within an error of at most 3%:

$$W(\theta_\gamma) = \sum_k c_k^{(2)} A_k P_k \left\{ \cos \left[ \theta_\gamma - \frac{1}{2}(\pi + \theta_p) \right] \right\}, \quad (2)$$

where  $A_k$  are the coefficients appropriate for a  $\gamma$ - $\gamma$  cascade:  $I(E2)I'(E2+M1)I''$ , and  $c_k^{(2)}$  are the "particle parameters" for spinless particles:

$$c_k^{(\lambda)} = 2\lambda(\lambda+1) / [2\lambda(\lambda+1) - k(k+1)] \quad \text{with } \lambda=2. \quad (3)$$

The angular distribution is therefore similar to one following the excitation of the nucleus by a spinless particle—the longitudinal photons of the Coulomb excitation process—carrying two units of angular momentum, and hitting the nucleus from a direction intermediate between  $\theta_p$  and  $\pi$ .

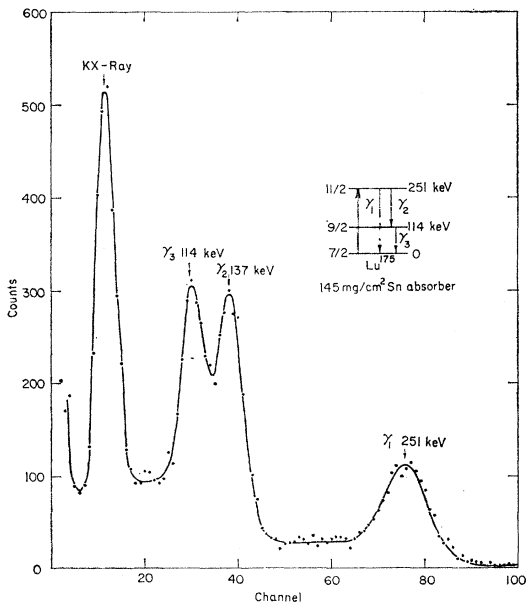


FIG. 6. Gamma-ray spectrum of  $\text{Lu}^{176}$  coincident with protons which leave the nucleus in the second excited level.

<sup>7</sup> K. Alder, A. Bohr, T. Huus, B. Mottelson, and A. Winther, *Revs. Modern Phys.* **28**, 432 (1956).

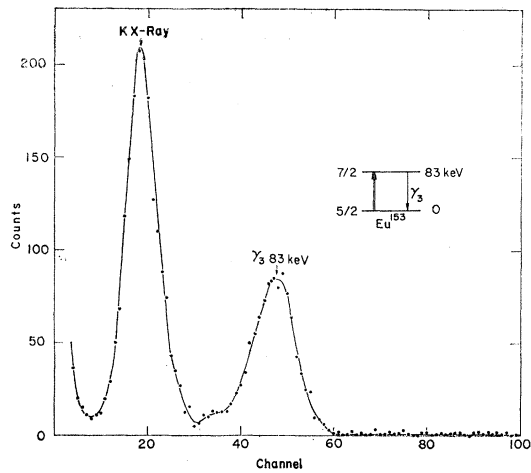


FIG. 7. Gamma-ray spectrum of  $\text{Eu}^{153}$  coincident with protons which leave the nucleus in the first excited level.

For the  $E1$  proton bremsstrahlung process,  $A_2 = \frac{1}{2}$ ,<sup>7</sup> and  $c_2^{(1)} = -2$  [from (3)]; therefore:

$$W(\theta_\gamma)_{\text{Br}} = 1 - P_2 \left\{ \cos \left[ \theta_\gamma - \frac{1}{2}(\pi + \theta_p) \right] \right\}, \quad (4)$$

the well-known dipole distribution.

The angular distribution (2) and (4) are much more anisotropic than those usually encountered in Coulomb excitation work with no restriction on the direction of the scattered protons. The anisotropy is however significantly reduced by the large angular aperture of the counter. The effect of the finite aperture can be represented as usual by "attenuation coefficients"  $B_k$ :

$$B_k = \int_x^1 P_k(x') \eta(x') dx' / \int_x^1 \eta(x') dx', \quad (5)$$

where  $x$  is the cosine of half the angle subtended by the counter at the target, and  $\eta(x) = \eta(\cos\theta)$  is the counter efficiency as a function of angle for radiation emitted from the target. The value of the angular distribution function for finite aperture  $\bar{W}(\theta_\gamma)$ , at the position of the

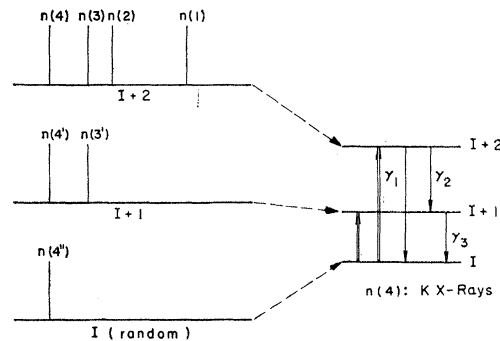


FIG. 8. Summary of notation used for the various gamma-ray transitions.

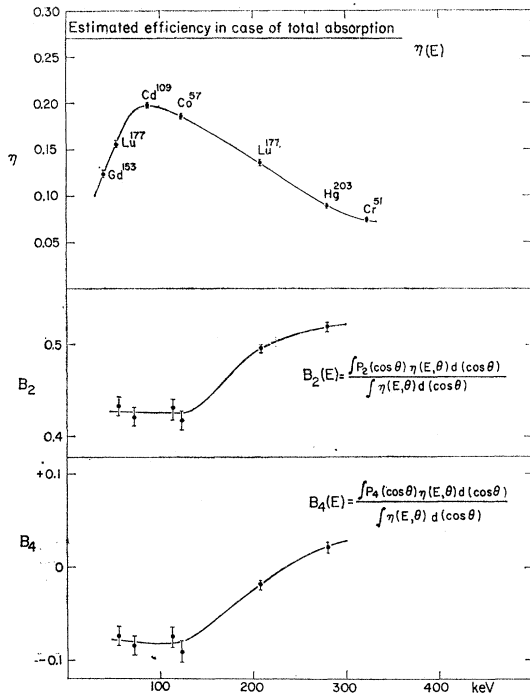


FIG. 9. Efficiency curves of the  $1\frac{1}{2}$ -in. diam, 1-in. high NaI crystal, with source 1 cm in front of the crystal. Upper part shows photopeak efficiency (not including escape peak). In the lower part the  $B_2$  and  $B_4$  attenuation coefficients are shown.

counter which we specify as  $\theta_\gamma = 0$ , is given by

$$\begin{aligned} \bar{W}(0) &= 1 + 2B_2A_2P_2(\cos\frac{7}{8}\pi) - \frac{3}{2}B_4A_4P_4(\cos\frac{7}{8}\pi), \\ \bar{W}(0)_{Br} &= 1 - B_2P_2(\cos\frac{7}{8}\pi). \end{aligned} \quad (6)$$

The values of  $A_2$ ,  $A_4$  depend on the mixing ratio  $\delta$ , and in the case of a transition  $I+1 \rightarrow I$  following the excitation of the  $I+2$  level (with the  $I+2 \rightarrow I+1$  transition unobserved),  $A_2$ , and  $A_4$  depend on the mixing ratios of both members of the cascade. It was found however that even with only a rough knowledge of the mixing ratios the value of  $\bar{W}(0)$  could be established with sufficient accuracy. The sign of  $\delta$  was in all cases taken from de Boer *et al.*<sup>8</sup> and Martin *et al.*<sup>9</sup>

### Calibrations

The efficiency of the gamma-ray counter for radiations of different energies was determined by placing radioactive sources in the exact position of the beam spot.

For the calibration of the sources a narrow pencil of radiation was produced by a tin-lined lead collimator, and this radiation was then registered by  $3 \times 3$ -in. NaI scintillator.

The sources used in these measurements were  $\text{Cr}^{51}$ ,

<sup>8</sup> J. de Boer, M. Martin, and P. Marmier, *Helv. Phys. Acta* **32**, 377 (1959).

<sup>9</sup> M. Martin, P. Marmier, and J. de Boer, *Helv. Phys. Acta* **31**, 435 (1958).

$\text{Co}^{57}$ ,  $\text{Cd}^{109}$ ,  $\text{Gd}^{153}$ ,  $\text{Lu}^{177}$ , and  $\text{Hg}^{203}$  which emit gamma rays and x rays of 323, 123, (22, 88), (41, 100), (55, 113, 208), and (72, 279) keV, respectively. Efficiency measurements were carried out separately for all the absorbers used in the experiments. The "full-energy" peak efficiency (without absorbers) is shown in Fig. 9 as a function of energy.

The attenuation coefficients  $B_2$ ,  $B_4$  were determined by measuring the angular dependence of the efficiency using a collimated beam of gamma rays which was played over the surface of the crystal. The attenuation coefficients  $B_2$ ,  $B_4$ , derived from such measurements, are shown in Fig. 9 as function of gamma-ray energy.

With the sources used for the efficiency calibrations, the spectral response of the scintillator to monoenergetic radiation could also be studied, and it was then established that the recorded gated gamma-ray spectra could be entirely resolved and analyzed in terms of radiation from four gamma-ray lines.

### Summation Peaks

If two gamma rays, or one gamma ray and a  $K$  x ray follow each other in a cascade, they may both register in the counter and produce a pulse, the height of which corresponds to the sum of their energies. There may, for example, be a contribution to the  $\gamma_1$  peak from a  $\gamma_2 + \gamma_3$  summation, and small peaks due to  $\gamma_2 + \gamma_4$ ,  $\gamma_3 + \gamma_4$  may appear. If the counting efficiencies and angular distribution for the various radiation are known, such summation peaks can be eliminated from the measured spectrum in a straightforward and unambiguous procedure.

### Interpretation

If the steps indicated in the last section are carried out, the number  $N(i)$  of photons  $\gamma_i$  ( $i=1-4$ ) emitted from the target over the whole sphere can be determined. Between the four numbers  $N(i)$  there exist three independent ratios and these have the following significance:

(1)  $N(1)/N(2)$  is the branching ratio for the two radiation  $\gamma_1/\gamma_2$ .

(2)  $N(2)/N(3)$  is equal to  $[1+\alpha(3)]/[1+\alpha(2)]$ , where  $\alpha(i)$  is the total conversion coefficient for the  $\gamma_i$  transition.

(3)  $N(4)/[N(2)+N(3)]$ . With a small and unambiguous correction for  $K$  conversion in the  $\gamma_1$  transition this ratio determines the quantity

$$f \frac{[1+\alpha(3)]\alpha_K(2) + [1+\alpha(2)]\alpha_K(3)}{2+\alpha(3)+\alpha(2)},$$

where  $\alpha_K(i)$  are the  $K$ -conversion coefficients, and  $f$  is the fluorescent yield.

If a coincidence measurement is also carried out for the first excited state, one gets the additional quantity:

(4)  $N(4')/N(3') = f\alpha_K(3)$ .

TABLE I. Ratios of various peaks in the coincidence spectra providing a general check on the measurements.

Nucleus	$\frac{1+\alpha(2)}{1+\alpha(3)}$		$\alpha_K(3)$		$\frac{[1+\alpha(3)]\alpha_K(2)+[1+\alpha(2)]\alpha_K(3)}{2+\alpha(2)+\alpha(3)}$	
	Meas.	Calc. <sup>a</sup>	Meas.	Calc. <sup>a</sup>	Meas.	Calc. <sup>a</sup>
<sup>63</sup> Eu <sup>153</sup>	0.48±0.07	0.53	2.47±0.20	2.38	1.37±0.36	1.56
<sup>73</sup> Ta <sup>181</sup>	0.82±0.14	0.72	1.64±0.46	1.40	1.24±0.51	1.05

<sup>a</sup> Derived from M. E. Rose, Internal Conversion Coefficients (North-Holland Publishing Company, Amsterdam, 1958) using  $\delta^2$  given in reference 3 for  $\gamma_3$ , and  $\delta^2$  from Table II for  $\gamma_2$ .

The ratios (2) to (4) can, in principle, be used to determine the mixing ratios for the  $\gamma_2$  and  $\gamma_3$  transitions, but the accuracy of such measurements is definitely inferior to measurements of, say,  $K/L$  ratio measurements, and the ratios (2) to (4) were used in the present experiments only as checks on the whole method. In Table I the values of  $\alpha_K(i)$  and  $[1+\alpha(2)]/[1+\alpha(3)]$  for Eu<sup>153</sup> and Ta<sup>181</sup> derived in this way are given and compared with values derived from conversion coefficient tables using  $\delta^2$  given in reference 3 for  $\gamma_3$ , and  $\delta^2$  from Table II for  $\gamma_2$ .

RESULTS AND DISCUSSION

The results of the measurements are summarized in Table II. The branching ratios here reported agree on the whole quite well with previous measurements. From the measured branching ratios  $\gamma_1/\gamma_2$  and from known values of  $B(E2)_1$  and  $\delta_2^2 = \{E2/M1\}_2$ , both transition probabilities for radiation No. 2— $B(E2)_2$  and  $B(M1)_2$ —can be evaluated separately.  $\delta^2$  is usually small, and

therefore—as has been pointed out before—this type of measurement is suitable particularly for determining magnetic transition probabilities whereas the accuracy of the electric transition probabilities is determined in the same cases by the accuracy with which  $\delta^2$  is known. The  $M1$  transition probabilities are expressed in Table II in terms of the quantity  $|g_R - g_K|_2$  as in reference 10. This is compared in column 8 with a similar quantity derived from the  $M1$  transition probability for transition No. 3 in Lu<sup>175</sup> and Ta<sup>181</sup>—two nuclei in which these quantities have been established by lifetime measurements. The values of  $|g_R - g_K|$  for the two transitions are seen to be very close and this verifies the basic stipulation of the collective rotation theory that these transition probabilities are related in the indicated manner and that the nuclear levels in question behave in this sense too as members of a rotational band. The parameter  $g_R, g_K$ —the gyromagnetic ratios of the collective rotation and of the intrinsic nuclear motion, respectively—are therefore definitely significant for de-

TABLE II. Summary of branching ratio measurements. The values  $B(M1)_2$  for transition No. 2 listed in column 6 and  $Q_0(2)$  in column 11 were computed from the branching ratios in column 2, the  $B(E2)_1$  values related to  $Q_0(1)$  in column 12, the  $\delta^2$  in column 4 and the energy ratios  $E(\gamma_2)/E(\gamma_1)$  in column 5.  $|g_R - g_K|_2$  in column 7 was computed from the  $B(M1)_2$  values, and  $|g_R - g_K|_3$  values for transition No. 3 are given in column 8 for comparison. The  $g_R$  values in column 10 are computed from  $|g_R - g_K|_2$  in column 7, and  $\mu$  in column 9. The energy ratios  $E(\gamma_2)/E(\gamma_1)$  in column 5 and the  $\mu$  values in column 9 are taken from a compilation by Bernstein *et al.*<sup>a</sup> The  $Q_0(2)$  values given in column 11 are compared with values of  $Q_0$  derived from the  $B(E2)$  values for transition No. 1 and No. 3.

1 Nucleus	2 Branching ratio from present work (crossover/cascade)	3 Branching ratio from previous work	4 $\delta^2$	5 $E(\gamma_2)/E(\gamma_1)$	6 $B(M1)_2$ ( $e\hbar/2Mc$ ) <sup>2</sup>	7 $ g_R - g_K _2$
<sup>63</sup> Eu <sup>153</sup>	2.84 ±0.18	1.62 <sup>b</sup> ; 2.0 <sup>c</sup> ; 1.3 <sup>d</sup>	0.47 ±0.07 <sup>e,e</sup>	0.568±0.012	0.0143±0.0018	0.175±0.011
<sup>64</sup> Gd <sup>155</sup>	0.344±0.024	0.26 <sup>b</sup> ; 0.21 <sup>c</sup>	0.035 $\begin{smallmatrix} +0.025^e \\ -0.018 \end{smallmatrix}$	0.590	0.116 ±0.017	0.779±0.061
<sup>64</sup> Gd <sup>157</sup>	0.271±0.027	0.27 <sup>b</sup> ; 0.36 <sup>c</sup>	0.040 $\begin{smallmatrix} +0.025^e \\ -0.016 \end{smallmatrix}$	0.584±0.009	0.131 ±0.019	0.827±0.062
<sup>68</sup> Er <sup>167</sup>	0.38 ±0.03	0.48 <sup>c</sup>	0.11 $\begin{smallmatrix} +0.13^e \\ -0.06 \end{smallmatrix}$	0.560±0.006	0.122 $\begin{smallmatrix} +0.015 \\ -0.020 \end{smallmatrix}$	0.391 $\begin{smallmatrix} +0.025 \\ -0.030 \end{smallmatrix}$
<sup>70</sup> Yb <sup>173</sup>	0.30 ±0.02	0.32 <sup>c</sup>	0.048 $\begin{smallmatrix} +0.034^e \\ -0.017 \end{smallmatrix}$	0.562±0.003	0.219 ±0.047	0.687±0.070
<sup>71</sup> Lu <sup>175</sup>	0.952±0.055	0.50 <sup>b</sup> ; 0.95 <sup>i</sup> ; 0.90 <sup>d</sup>	0.21 ±0.03 <sup>e,i</sup>	0.548	0.0903±0.0014	0.336±0.025
<sup>72</sup> Hf <sup>177</sup>	5.59 ±0.73	2.62 <sup>b</sup> ; 3.8 <sup>c</sup> ; 4.3 <sup>d</sup>	10 $\begin{smallmatrix} +14^e \\ -5 \end{smallmatrix}$	0.548	0.0014 $\begin{smallmatrix} +0.0012 \\ -0.0008 \end{smallmatrix}$	0.042±0.016
<sup>73</sup> Ta <sup>181</sup>	0.694±0.050	0.36 <sup>b</sup> ; 0.82 <sup>i</sup> ; 0.57 <sup>m</sup> 0.66 <sup>n</sup> ; 0.69 <sup>o</sup>	0.19 ±0.04 <sup>e,i,p</sup>	0.548	0.152 ±0.020	0.437±0.028

TABLE II (continued).

1	8	9	10	11	12	13	
Nucleus	$ g_R - g_K _3$	$\mu = [I/(I+1)](g_R + I g_K)$ ( $e\hbar/2Mc$ )	odd- $N$	$g_R$ odd- $Z$	$Q_0(2)$ ( $10^{-24}$ cm $^2$ )	$Q_0(1)$ ( $10^{-24}$ cm $^2$ )	$Q_0(3)$ ( $10^{-24}$ cm $^2$ )
$^{63}\text{Eu}^{163}$		$1.507 \pm 0.002$		$0.477 \pm 0.008$	$5.20 \pm 0.44$	$6.54 \pm 0.18^f$	$6.98 \pm 0.15^f$
$^{64}\text{Gd}^{155}$		$-0.28 \pm 0.03$	$0.280 \pm 0.047$		$6.05 \pm 1.82$	$6.33 \pm 0.42^e$	$6.53 \pm 0.15^e$
$^{64}\text{Gd}^{157}$		$-0.37 \pm 0.04$	$0.249 \pm 0.055$		$7.7 \begin{smallmatrix} +2.1 \\ -1.8 \end{smallmatrix}$	$6.58 \pm 0.27^e$	$6.62 \pm 0.15^e$
$^{68}\text{Er}^{167}$		$-0.5 \pm 0.1$	$0.161 \begin{smallmatrix} +0.035 \\ -0.038 \end{smallmatrix}$		$7.5 \begin{smallmatrix} +3.2 \\ -2.4 \end{smallmatrix}$	$7.50 \pm 0.25^f$	$7.86 \pm 0.12^f$
$^{70}\text{Yb}^{173}$		$-0.665 \pm 0.01$	$0.225 \pm 0.051$		$7.0 \begin{smallmatrix} +2.1 \\ -1.7 \end{smallmatrix}$	$7.37 \pm 0.74^h$	$7.82 \pm 0.39^h$
$^{71}\text{Lu}^{175}$	$0.340 \pm 0.014^j$	$2.0 \pm 0.2$		$0.309 \pm 0.060$	$6.50 \pm 0.59$	$7.31 \pm 0.50^k$	$7.51 \pm 0.16^k$
$^{72}\text{Hf}^{177}$		$0.61 \pm 0.03$	$0.207 \pm 0.016$		$5.68 \begin{smallmatrix} +0.47 \\ -0.57 \end{smallmatrix}$	$6.79 \pm 0.34^l$	$6.75 \pm 0.18^l$
$^{72}\text{Ta}^{181}$	$0.460 \pm 0.020^j$	$2.340$		$0.329 \pm 0.021$	$6.68 \pm 0.70$	$6.72 \pm 0.34^q$	$7.04 \pm 0.17^q$

<sup>a</sup> See reference 11.

<sup>b</sup> N. P. Heydenburg and G. M. Temmer, Phys. Rev. **104**, 981 (1956).

<sup>c</sup> See reference 8.

<sup>d</sup> G. Goldring and G. T. Paulissen, Phys. Rev. **103**, 1314 (1956).

<sup>e</sup> See reference 3.

<sup>f</sup> See reference 4.

<sup>g</sup> V. Ramšak, M. C. Olesen, and B. Elbek, Nuclear Phys. **6**, 451 (1958).

<sup>h</sup> B. Elbek, K. O. Nielsen, and M. C. Olesen, Phys. Rev. **108**, 406 (1957).

<sup>i</sup> See reference 9.

<sup>j</sup> See reference 2.

<sup>k</sup> B. Elbek, M. C. Olesen, and O. Skilbreid, Nuclear Phys. **10**, 294 (1959).

<sup>l</sup> O. Hansen, M. C. Olesen, O. Skilbreid, and B. Elbek, Nuclear Phys. **25**, 634 (1961).

<sup>m</sup> P. H. Stelson and F. K. McGowan, Phys. Rev. **99**, 112 (1955).

<sup>n</sup> R. H. Davis, A. S. Divatia, D. A. Lind, and R. D. Moffat, Phys. Rev. **103**, 1801 (1956).

<sup>o</sup> E. A. Wolicki, L. W. Fagg, and E. H. Geer, Phys. Rev. **105**, 238 (1957).

<sup>p</sup> F. K. McGowan and P. H. Stelson, Phys. Rev. **109**, 901 (1958).

<sup>q</sup> O. Hansen (private communication).

scribing the magnetic dipole properties in this region. In column 10  $g_R$  is computed according to reference 10 from the ground-state magnetic moment:

$$\mu = [I/(I+1)](g_R + I g_K),$$

where  $I$  is the ground-state spin, and from  $|g_R - g_K|$  as determined from the  $M1$  transition probabilities. A striking feature of the systematic behavior of  $g_R$  is that this quantity is definitely and consistently smaller for odd- $N$  nuclei than for odd- $Z$  nuclei. This fact has already been noticed previously by Bernstein and de Boer<sup>11</sup> and commented on by Nilsson and Prior.<sup>1</sup> The values of  $g_K$  were found to be in good agreement with the predictions of the Nilsson model. As  $g_K$  is insensitive to the exact values of  $B(M1)$ , neither new information nor accuracy is gained in this case in the present measurements.

<sup>10</sup> A. Bohr and B. R. Mottelson, Kgl. Danske Videnskab. Selskab. Mat.-fys. Medd. **27**, No. 16 (1953).

<sup>11</sup> E. M. Bernstein and J. de Boer, Nuclear Phys. **18**, 40 (1960).

The  $E2$  transition probabilities for  $\gamma_2$  are expressed in column 11 in terms of the intrinsic quadrupole moment  $Q_0(2)$ . This is compared with  $Q_0$  values for transitions 1 and 3, and here too—in agreement with previous measurements—we find the  $Q_0$  values for the various transitions to be generally consistent. The  $Q_0$  values for transition 2 are on the average some 15% lower than the  $Q_0$  values for the other two transitions, but the difference is hardly significant.

#### ACKNOWLEDGMENTS

We are greatly indebted to Dr. Cotton from the Centre d'Etudes Nucléaires de Saclay for his cooperation and assistance in getting this experiment started and carried out at the Van de Graaff laboratory in Saclay. Our sincere thanks are due to M. Picou for taking part in the early stages of this work, to Mlle. Doury for her help in preparing the targets, and to the staff of the Saclay Van de Graaff for their cooperation all through the long hours of this experiment.